Authors run-on-prints of the journal

INTERNATIONAL POLYMER PROCESSING

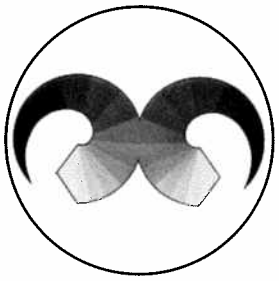

POLYMER PROCESSING SOCIETY

V. Kumar and J. E. Weller*

Department of Mechanical Engineering, University of Washington, Seattle, U.S.A.

A Process to Produce Microcellular PVC

A novel process to produce microcellular PVC foams with a very homogeneous cell distribution and cell densities ranging from 10^7 to 10^9 cells/cm^3 is described. Microcellular PVC foams with relative densities (density of foam divided by the density of unfoamed polymer) ranging from 0.15 to 0.94 have been produced. In this paper, experimental results on bubble nucleation and growth are presented. It was found that the bubble nucleation density increases with foaming temperature and eventually reaches a limiting value, while the average bubble diameter is relatively independent of the foaming temperature. A majority of the cell growth was found to occur in the early stages of foaming.

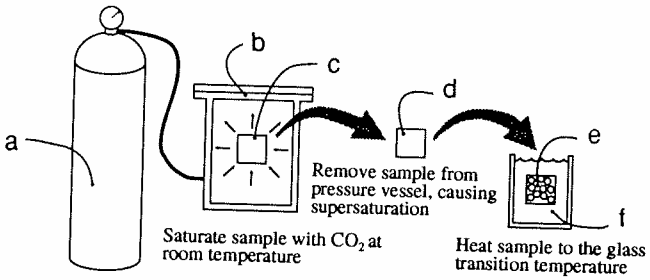

Fig. 1. Schematic of the process to produce microcellular PVC a: carbon dioxide cylinder, b: pressure vessel, c: original sample, d: supersaturated sample, e: foamed sample, f: glycerin bath with temperature control

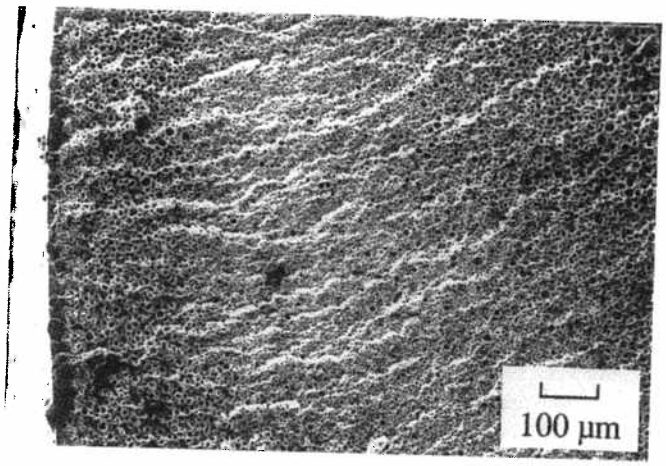

Fig. 2. Scanning electron micrograph of microcellular PVC, showing a homogeneous structure across the thickness

1 Introduction

Very homogeneous microcellular foams, with an average cell size of the order of 10 μm can be produced in PVC in a two stage process. In the first stage, a PVC sample absorbs carbon dioxide in a pressure vessel, maintained at 4.8 MPa (700 psi) and room temperature. In the second stage, the saturated sample is removed from the pressure vessel and heated to the glass transition temperature, causing cell nucleation and growth. The saturated samples may be heated to a temperature higher than the glass transition temperature to produce foams of lower density. Such a process was first developed by Martini, Suh, and Waldman [1] as a means to reduce the amount of plastics used in mass produced items. The basic process to produce mocrocellular plastics is discussed by Martini et al. [1], who used nitrogen to create a microcellular structure in polystyrene. The bubble nucleation, growth, and processing issues in the polystyrene-nitrogen system have been studied by a number of investigators [2 to 7]. Recently, Kumar and coworkers have reported results on microcellular polycarbonate [8 to 10].

Fig. 1 shows a schematic of the process to produce microcellular PVC. The process uses carbon dioxide which was chosen because of its high solubility in PVC [11, 12], and thus the potential to produce a high cell nucleation density. A scanning electron micrograph of microcellular PVC is shown in Fig. 2. The micrograph shows a very uniform nucleation of bubbles across the sample thickness. The left edge in Fig. 2 shows a skin region with no bubbles that is approximately 25 μm in thickness. The thickness of this skin region can be controlled by allowing the carbon dioxide to escape from the saturated sample surfaces for a predetermined length of time prior to heating [13]. The small cell size and high cell density in microcellular foams provide the possibility to foam thin wall parts in the 0.5 to 2 mm range, which can not be produced with conventional processes since the fewer and larger cells produced by these processes cause an excessive loss of strength. Further, the homogeneous microstructure of microcellular PVC foams is expected to reduce the variability in foam properties, in contrast with structural foams that are typically characterized by a large variation in structure across the thickness [14].

In this paper, we describe the process to produce microcellular PVC, and present experimental results on the relationship between some of the key process parameters.

* Mail address: Prof. Dr. V. Kumar, Department of Mechanical Engineering, Mail Stop FU-10, University of Washington, Seattle, Washington 98195, U.S.A.

2 Experimental

A rigid, transparent PVC formulation provided by the BFGoodrich Company is the form of molded sheets with an approximate thickness of 2 mm and a glass transition temperature of 78.2 °C was used. The density of this material was measured to be 1.33 g/cm^3. The sheets were cut into 3 cm × 3 cm squares and placed in a pressure vessel connected to a CO_2 cylinder. The samples were then saturated with CO_2 gas at 4.8 MPa (700 psi) and 22 °C. During saturation, the samples were periodically removed from the pressure vessel and weighed on a precision balance with an accuracy of 10 μg. Because the amount of gas absorbed by the samples was on the order of 10 mg, this method of monitoring gas sorption provided sufficient accuracy. Upon saturation, the samples were removed from the pressure vessel and immediately foamed. The samples in this experiment were foamed in a glycerin bath maintained at the desired foaming temperature for a predetermined length of time. The temperature used to foam the samples, and the amount of time the samples were held at this temperature will be referred to as the foaming temperature and foaming time respectively. After foaming, the samples were placed in liquid nitrogen and fractured. The fractured surface, exposing the internal microstructure, was made conductive by deposition of Au-Pd vapor, and then the samples were studied using scanning electron microscopy (SEM). From the micrographs, the cell nucleation density and the average cell size were determined. All micrographs were taken near the center of the sample cross section.

The number of cells nucleated per unit volume of the original polymer is called the cell density, N_o. The cell density is determined by dividing the number of cells per unit volume of foam by the volume of polymer in a unit volume of foam. The number of cells per cm^3 of foam, N_f, can be determined from a SEM micrograph containing 100 to 200 cells. If the area of the micrograph is A, then the actual area is given by A/M^2, where M is the magnification of the micrograph. Thus, the area cell density is the number of cells in the micrograph, n, divided by the actual area. The line cell density is the number of cells per unit of foam and is simply the square root of the area density. Assuming that the cell distribution in the foam is homogeneous and isotropic, the number of cells nucleated per cm^3 of foam N_f can be estimated by cubing the line density:

$$N_f = \left(\frac{nM^2}{A}\right)^{3/2} \tag{1}$$

where n = number of cells in the micrograph, M = magnification of the micrograph, A = area of the micrograph (cm^2), N_f = the number of cells per cm^3 of foam.

The volume of polymer per cm^3 of foam is $(1 - V_f)$, where V_f is the void fraction of the foam. The void fraction, or volume occupied by the voids per cm^3 of foam can be estimated by multiplying the volume of an average cell by the number of cells per cm^3 of the foam. If D is the average diameter of the cells, obtained from averaging the major and minor diameters of 25 to 50 cells in a SEM micrograph, then:

$$V_f = \frac{\pi D^3}{6} N_f. \tag{2}$$

Thus, the number of cells nucleated per cm^3 of original volume of polymer, N_o, is:

$$N_o = \frac{N_f}{(1 - V_f)}. \tag{3}$$

The cell density reported in this paper is as given by Eq. 3.

3 Results and discussion

3.1 Sorption of CO_2 in PVC and its effect on the glass transition

Fig. 3 shows a plot of the CO_2 uptake in mg CO_2 per g of polymer as a function of time for a saturation pressure of 4.8 MPa (700 psi). We see that the concentration at equilibrium reaches approximately 75 mg CO_2/g of PVC, or 7.5 % by weight. Because of this high CO_2 concentration, we would expect significant plasticization of the polymer to occur, resulting in a lower glass transition temperature. A theoretical model has been developed to predict the glass transition in polymer-diluent systems by Chow [15], and has been shown to be in good agreement with experimental data [16]. According to this model, the glass transition temperature is given by

$$\ln\left(\frac{T_g}{T_{go}}\right) = \beta[(1 - \theta)\ln(1 - \theta) + \theta \ln(\theta)] \tag{4}$$

where

$$\beta = \frac{zR}{M_p \Delta C_{pp}}, \tag{5}$$

$$\theta = \frac{M_p}{zM_d} \frac{\omega}{1 - \omega}. \tag{6}$$

ω = mass fraction of diluent, M_p = molecular weight of the monomer, M_d = molecular weight of the diluent, R = gas constant, T_{go} = glass transition of the pure polymer, T_g = reduced glass transition, z = coordination number, ΔC_{pp} = excess transition isobaric specific heat of the polymer.

For PVC, Chiou et al. [16] suggest a $\Delta C_{pp} = 0.0693$ cal/g °C. The glass transition of the pure PVC formulation used in this experiment was 78.2 °C. In addition, Chow [15] recommends a value of z = 2, based on comparison with

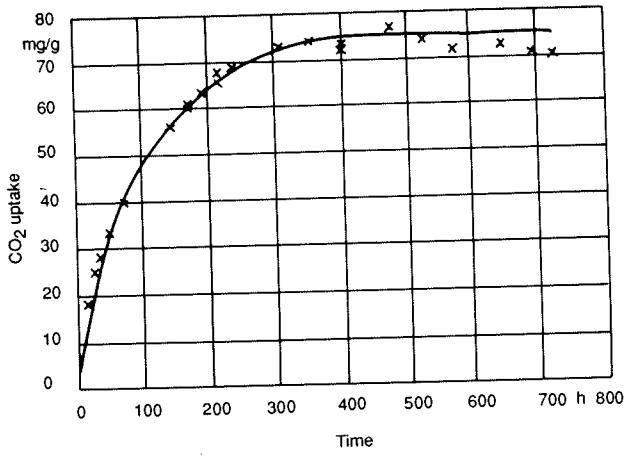

Fig. 3. Sorption curve for PVC in CO_2 at 4.8 MPa (700 psi) and 22 °C

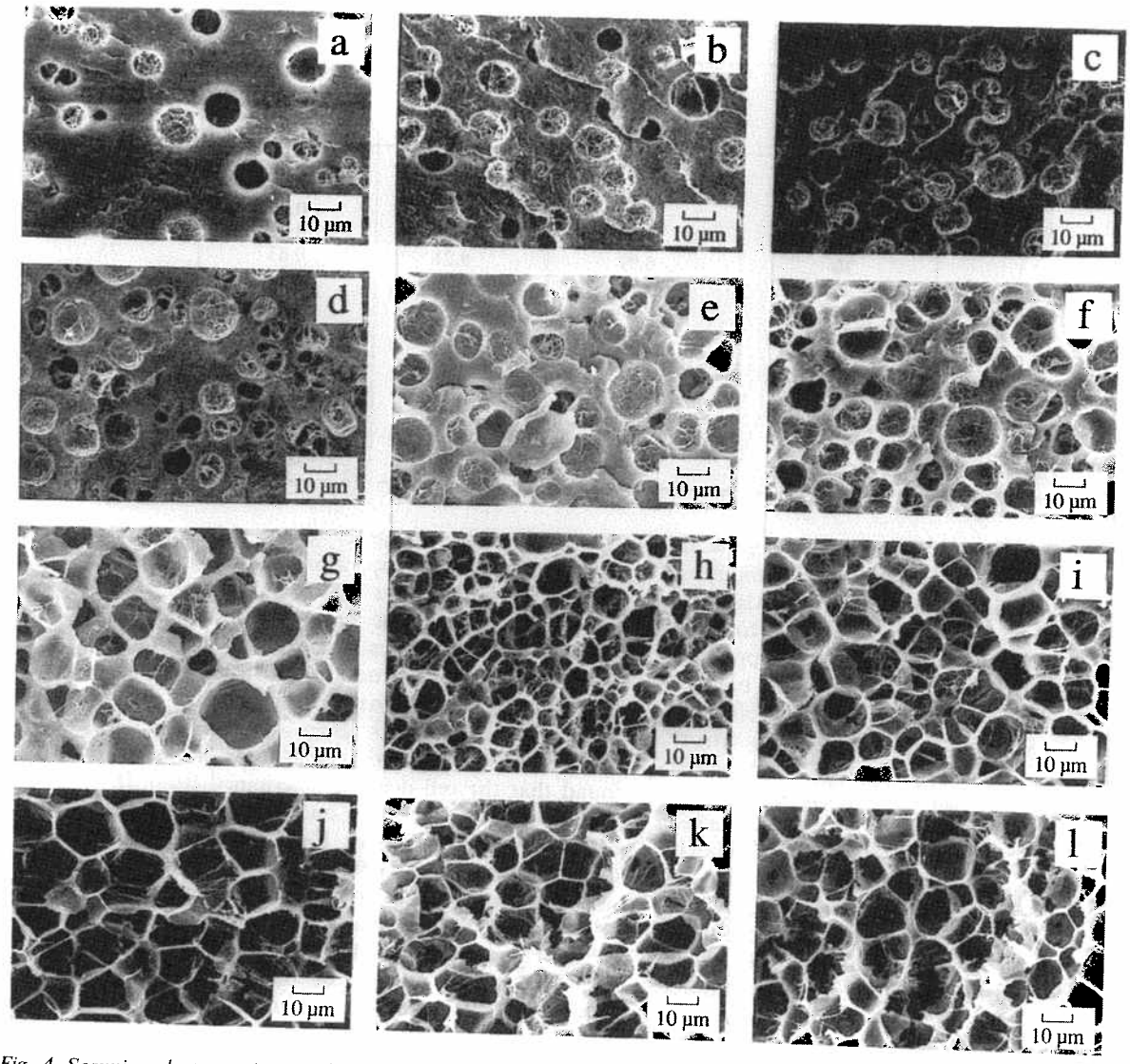

Fig. 4. Scanning electron micrographs of microcellular PVC foamed at different temperatures
a: 56 °C, b: 61 °C, c: 65 °C, d: 70 °C, e: 75 °C, f: 80 °C, g: 90 °C, h: 95 °C, i: 100 °C, j: 105 °C, k: 110 °C, l: 115 °C

experimental data. From Fig. 3 we can see that at equilibrium, the concentration of CO_2 is approximately 75 mg/g, thus $\omega = 0.075$. Using the above values, the predicted T_g of PVC, saturated with a CO_2 concentration of 75 mg/g is approximately 14 °C. In the original microcellular process [1], supersaturated polystyrene sheets were heated to the glass transition of the pure polymer. However, in light of the depression of the glass transition at high CO_2 concentrations, we expect bubbles to nucleate at temperatures significantly below the T_g of the pure polymer.

3.2 Effect of temperature on cell nucleation and growth

We investigated the effect of foaming temperature on cell nucleation and growth by foaming samples for 30 s at subsequently higher temperatures. When a sample is heated, foaming becomes evident as the sample turns white. This visual observation of bubble nucleation and growth was possible since we were using a clear, transparent formulation of PVC. As the bubbles grow to a size where light can be diffracted, the sample becomes opaque. The samples foamed at 40, 45, and 50 °C did not 'turn white,' and were therefore considered to not have foamed in our context. The first visible foam was produced at 156 °C. Samples were then foamed at 5 °C intervals up to a temperature of 120 °C. This broad range of temperatures was employed to investigate the effect of foaming temperature on the foam microstructure and the resulting foam density. Fig. 4 shows SEM micrographs of PVC foamed at increasing temperatures. All micrographs were taken at a magnification of 1000× in order to allow a visual evaluation of the effect of foaming temperature on the microstructure. Table 1 summarizes the experimental conditions, the cell sizes, and cell densities determined from the micrographs for this experiment. As expected, we can see that nucleation has occurred at temperatures significantly below the original glass transition temperature, and that a microcellular structure can be achieved within the range of foaming temperatures explored.

Table 1. Experimental conditions and results at increasing foaming temperature

Ps MPa	Foaming temp. °C	Foaming time s	$N_o \times 10^{-8}$ cells/cm³	D μm	Foam density g/cm³	CO_2 uptake mg/g
4.8	56.0	30	0.20	9.22	1.22	75
4.8	60.6	30	0.84	10.29	1.03	75
4.8	65.2	30	2.48	9.38	0.96	75
4.8	70.1	30	2.70	10.00	0.79	75
4.8	75.1	30	6.99	9.21	0.63	75
4.8	80.2	30	7.95	9.90	0.53	75
4.8	84.8	30	9.56	10.13	0.47	75
4.8	89.9	30	18.1	8.36	0.32	75
4.8	95.0	30	55.9	8.63	0.32	75
4.8	100.0	30	41.3	8.46	0.29	75
4.8	105.0	30	10.3	13.16	0.21	75
4.8	110.0	30	7.99	10.12	0.25	75
4.8	115.0	30	14.3	10.50	0.25	75
4.8	120.0	30	27.98	7.36	0.40	75

We can also see that for samples a through f, there is an increasing number of bubbles in the micrographs, implying that the cell density is increasing with temperature. Also note that for samples a through f, corresponding to a foaming temperature range of 56 °C to 80 °C, the bubbles appear to be spherical. At higher foaming temperatures the bubbles begin to touch each other and a honeycomb-type of structure develops. Fig. 5 is a plot of the cell nucleation density as a function of the foaming temperature. Note that the cell density in number of cells per cm³ of original polymer has been plotted on a log scale. From Fig. 5 we see that the cell density increases between 56 °C and 90 °C by approximately two orders of magnitude. The data in Fig. 5 also suggests that the increase in cell density with temperature occurs at an ever decreasing rate, until the cell density levels off at approximately 2×10^9 cells/cm³ for temperatures above 90 °C. It appears that above 90 °C the coalescence of bubbles acts to counterbalance any increase in bubble nucleation, leading to a cell density that is nearly constant with further rise in temperature. Another factor that may contribute to the cell density reaching a limiting value is that the growth of smaller cells is hampered by the growth of larger cells that have nucleated earlier. Since the pressure inside a larger cell is smaller, the gas concentration gradient in the vicinity of a larger cell is higher, thus favoring the diffusion of available gas into the larger cell as apposed to a neighboring smaller one. Thus larger cells grow at the expense of smaller ones, until an equilibrium structure is established.

It should be noted that the data in Fig. 5 is a snapshot of foam microstructures taken at a fixed foaming time of 30 s. In an experiment on cell growth, discussed below, we found that the cell density, determined from SEM micrographs, reduces by nearly one order of magnitude in the first 60 s of foaming (see Fig. 10). The decrease in cell density within the first 30 s of foaming is nearly two thirds of the decrease seen in 60 s. This decrease in cell density as a function of foaming time is attributed to the phenomenon of bubble coalescence that accompanies bubble growth. Thus the actual number of bubbles nucleated per unit volume of PVC could be up to an order of magnitude higher than reported in Fig. 5 due to bubbles lost to coalescence, and therefore not counted.

The average cell diameter is plotted in Fig. 6 as a function of foaming temperature. We can see that over the

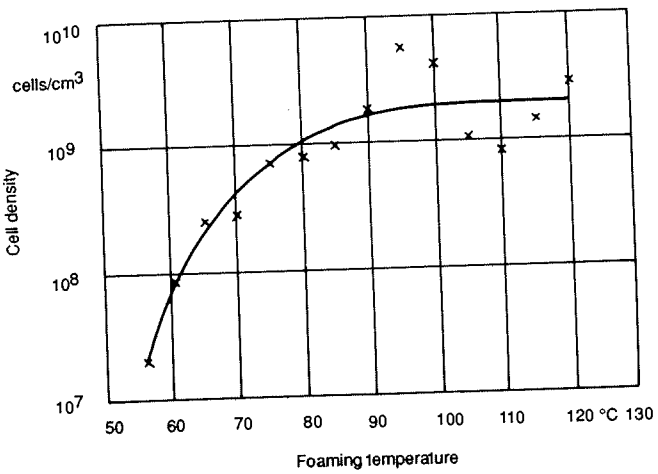

Fig. 5. Plot of cell density as a function of foaming temperature

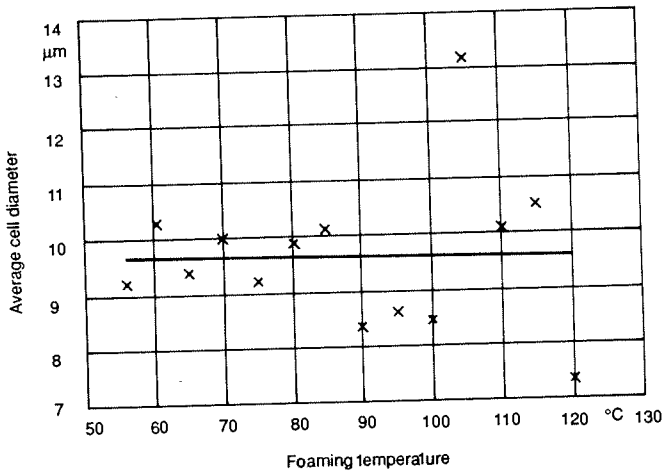

Fig. 6. Plot of average cell diameter as a function of foaming temperature

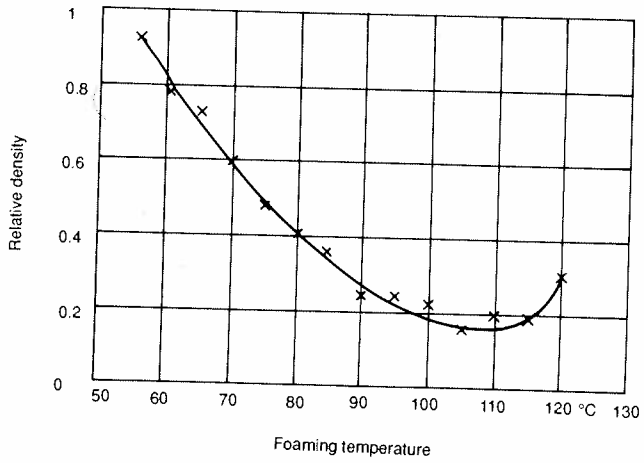

Fig. 7. Plot of foam relative density as a function of foaming temperature

range of foaming temperatures explored, the average cell diameter remains fairly constant. This behavior is counter intuitive to what we would expect; as the foaming temperature goes up, the polymer viscosity decreases, allowing the cells to grow larger. However, cell growth must compete with cell nucleation for the available gas. Since the cell density increases with foaming temperature, more cells are being formed at the expense of cell growth, keeping the average bubble size early constant.

The foam density is plotted in Fig. 7. We can see that density decreases linearly as the foaming temperature is increased, from 56 °C to 90 °C. This decrease in density is consistent with an increasing cell density and the relatively constant cell diameter over this temperature range. Beyond 90 °C, the foam density decreases with temperature in a nonlinear fashion, and goes through a minimum at approximately 105 °C. It appears that above 105 °C the diffusivity of CO_2 has increased to a point where some of the gas diffuses out of the sample instead of supporting cell nucleation and growth. From Fig. 7 we can also see that the relative density has dropped to approximately 0.15 at 105 °C, an 85 % reduction in the density of the original PVC.

3.3 Rate of cell growth

The rate of cell growth is an important process parameter. The cell growth rate is a complex function of the viscosity and surface tension of the polymer, and the solubility and diffusivity of the gas within the matrix. To determine the rate of cell growth in the PVC-CO_2 system, samples were foamed at 75 °C for increasing foaming times, ranging from 10 s to a maximum foaming time of 4 min. The foaming temperature of 75 °C was chosen based on the previous experiment, corresponding to a relative density of 50 %, for 30 s of foaming time, as shown in Fig. 7. Fig. 8 shows micrographs of microcellular PVC samples foamed at in-

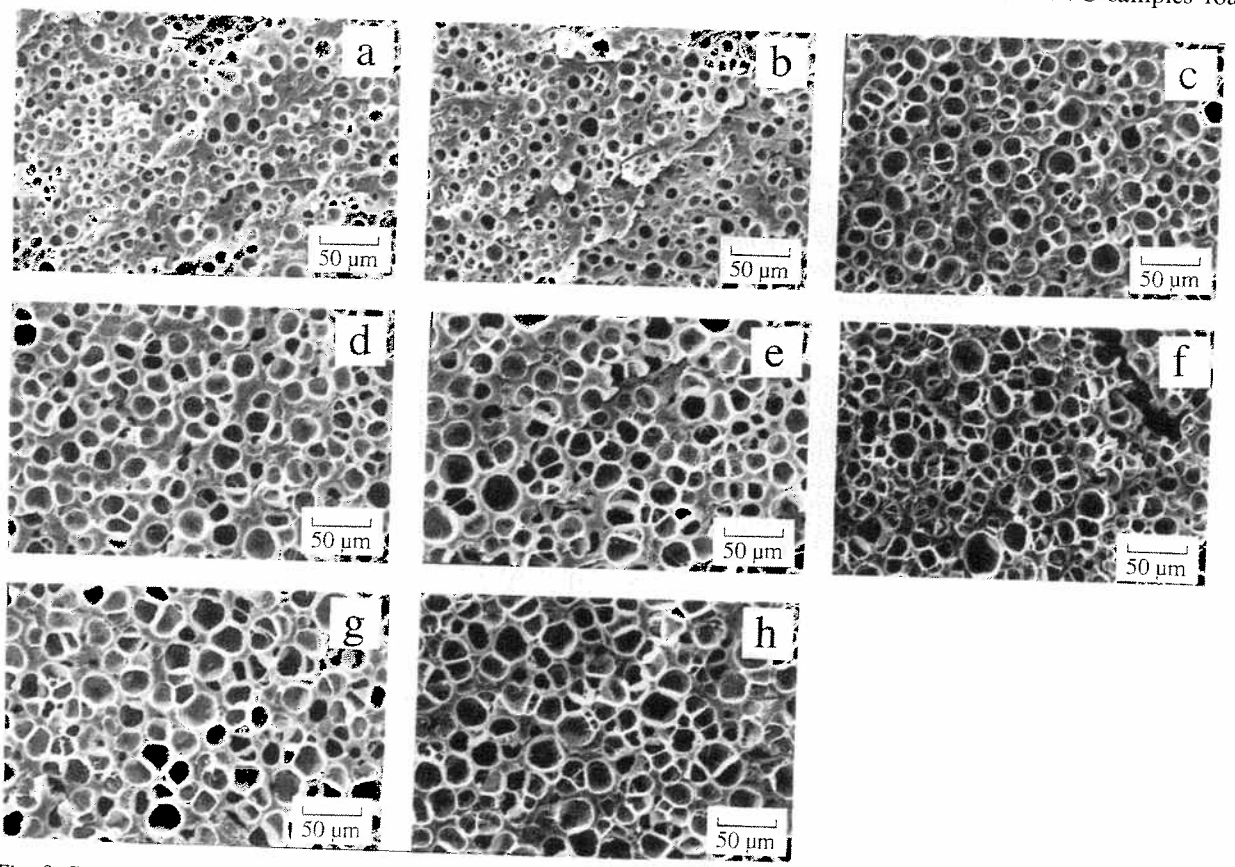

Fig. 8. Scanning electron micrographs of microcellular PVC foamed at different times a: 10 s, b: 20 s, c: 30 s, d: 40 s, e: 60 s, f: 90 s, g: 120 s, h: 240 s

Table 2. Experimental conditions and results at increasing foaming times

Ps MPa	Foaming temp. °C	Foaming time s	$N_o \times 10^{-8}$ cells/cm^3	D μm	Foam density g/cm^3	CO_2 uptake mg/g
4.8	75.0	10	15.78	4.36	0.91	75
4.8	75.0	20	8.38	6.32	0.79	75
4.8	75.0	30	3.33	11.16	0.65	75
4.8	75.0	40	1.74	16.05	0.61	75
4.8	75.0	60	1.92	19.30	0.56	75
4.8	75.0	90	2.29	14.08	0.50	75
4.8	75.0	120	1.65	18.56	0.47	75
4.8	75.0	240	1.13	18.13	0.46	75

creasing foaming times. Again, to faciliate a visual comparison, all micrographs in Fig. 8 were taken at constant magnification of 350×. We see that the bubbles increase in size as we go from micrograph a to d, beyond which there is not much change in the microstructure. Table 2 summarizes the experimental conditions, the cell sizes, and cell densities determined from the micrographs.

The average cell diameter is plotted in Fig. 9 as a function of the foaming time. We can see that the average cell size grows rapidly in the first 50 s and then reaches a limiting value of approximately 18 μm after the driving force for growth has been depleted. The cell density as a function of the foaming time is plotted in Fig. 10. We can see that within the first 60 s, the cell density drops by approximately one order of magnitude due to bubble coalescence.

The cell density and average cell diameter determine the void fraction, and thus the density of the foam. The measured relative density is plotted as a function of foaming time in Fig. 11. We can see that the relative density approaches a limiting value after approximately 100 s, which is consistent with the data shown in Figs. 9 and 10. We note also that for a foaming time of 30 s in this experiment, a relative density of 0.49 is obtained, which is consistent with the data in Fig. 7.

4 Conclusions

We have presented details of a process to produce microcellular PVC foams with a wide range of foam relative densities. In this study, foam relative densities obtained ranged from 0.15 to 0.94. The following conclusions can be drawn regarding the PVC-CO_2 system:

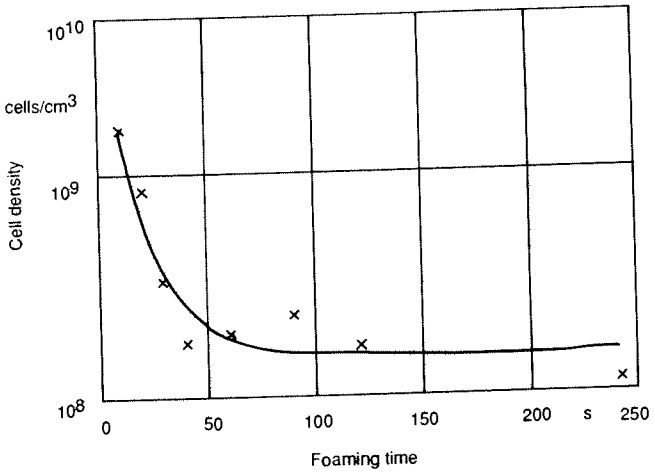

Fig. 10. Plot of cell density as a function of foaming time

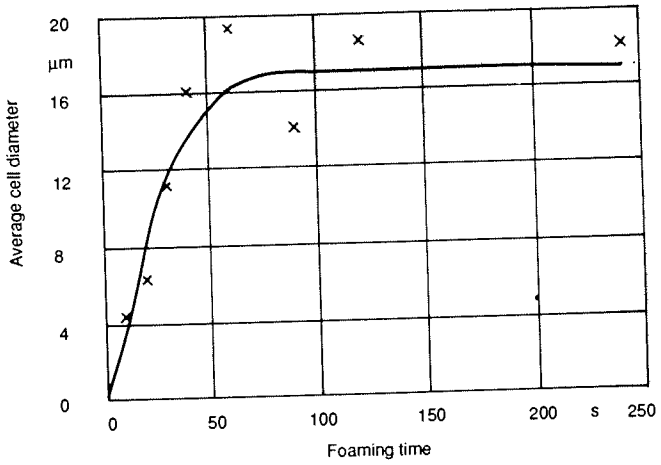

Fig. 9. Plot of average cell diameter as a function of foaming time

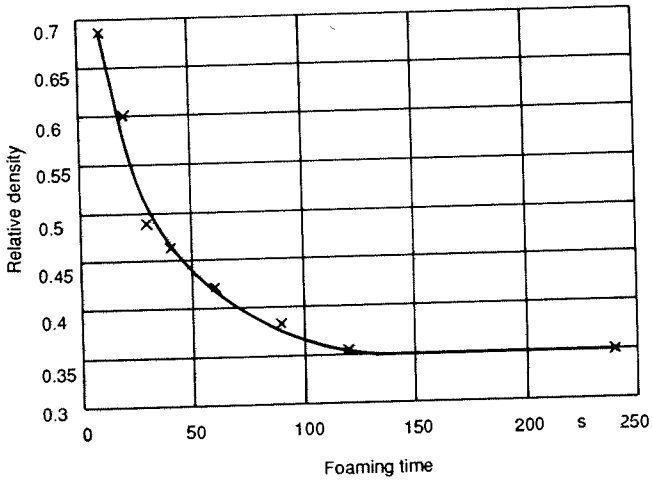

Fig. 11. Plot of foam relative density as a function of foaming time

1) Bubble nucleation and growth can occur at temperatures well below the glass transition temperature of the original polymer due to plasticization of PVC by CO_2. The lowest temperature at which microcellular PVC could be produced was found to be 56 °C.
2) The bubble nucleation density appears to increase with temperature in the range 56 °C to 90 °C, and tends to level off with further increase in foaming temperature.
3) The density of microcellular PVC decreases monotonically with temperature in the range of 56 °C to 105 °C. Therefore, accurate control of the foam density is possible by controlling the foaming temperature.
4) Much of the cell growth takes place within the first 60 s of foaming. Beyond this time, the foam structure does not appear to change significantly. A foaming time of 20 to 30 s is adequate to obtain bubbles of approximately 10 μm in diameter.

We believe that the discovery of microcellular PVC has the potential to significantly impact the vinyl industry. Microcellular PVC with relative densities in the 0.7 to 0.9 range may be able to replace solid PVC now used in a number of applications, offering significant reduction in materials costs. In lower relative density ranges, microcellular PVC is expected to offer a new range of properties to the engineer due to its extremely homogeneous microstructure.

Nomenclature

A	area of a micrograph, cm^2
$\mathscr{D}$	diffusion coefficient, cm^2/s
ΔC_{pp}	excess transition isobaric specific heat of the polymer, cal/g °C
ℓ	sample thickness, cm
M	magnification of a micrograph
M_d	molecular weight of the diluent
M_p	molecular weight of the monomer
M_t	amount of gas remaining in the polymer at time t, g
M_∞	amount of gas at equilibrium saturation, g
n	number of cells in a micrograph
N_f	the number of cells per cm^3 of foam
R	gas constant
t	elapsed time in seconds
T_g	reduced glass transition, K
T_{go}	glass transition of the pure polymer, K
ω	mass fraction of diluent
z	coordination number

Appendix A: Diffusivity of carbon dioxide in PVC

The diffusivity of carbon dioxide in PVC was measured in a desorption experiment. A PVC sample, 2.05 mm thick, was saturated with CO_2 maintained at 4.8 MPa (700 psi) and 22 °C. The sample was then withdrawn from the pressure vessel and weighed periodically until the amount of carbon dioxide remaining in the sample was approximately 80 % of the value at saturation. For early states of diffusion of gas from the sample, the amount of gas remaining in a plane sample at any time is related to the diffusion coefficient by [17]

$$\frac{M_t}{M_\infty} = 1 - \frac{4}{\sqrt{\pi}}\left(\frac{\mathscr{D}t}{\ell^2}\right)^{1/2} \qquad \text{(A1)}$$

where M_t = amount of gas remaining in the polymer at time t, g, M_∞ = amount of gas at equilibrium saturation, g, $\mathscr{D}$ = diffusion coefficient, cm^2/s, ℓ = sample thickness, cm, t = elapsed time, s.

If M_t/M_∞ is plotted against $\sqrt{t/\ell^2}$, then the slope R is given by

$$R = \frac{4\sqrt{\mathscr{D}}}{\sqrt{\pi}}, \qquad \text{(A2)}$$

and the diffusion coefficient can be found from

$$\mathscr{D} = \frac{\pi R^2}{16}. \qquad \text{(A3)}$$

Fig. A1 shows a plot of M_t/M_∞ as a function of $\sqrt{t/\ell^2}$ for our desorption experiments. From this data an average diffusion coefficient for carbon dioxide–PVC system was determined to be 1.3×10^{-8} cm^2/s.

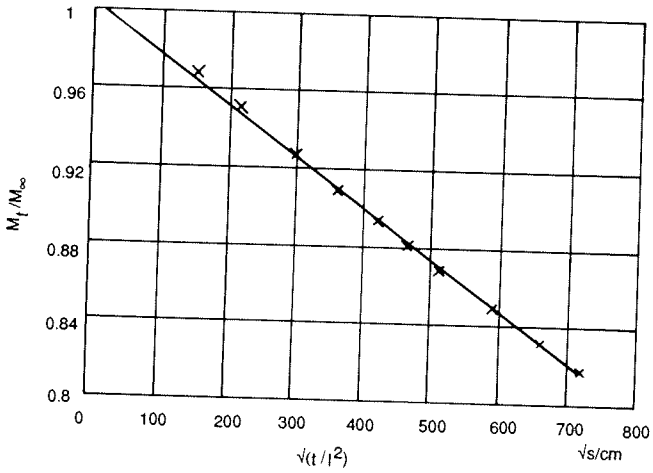

Fig. A1. Desorption plot for the PVC–carbon dioxide system

6 References

1 US Patent 4 473 665 (1984) *Martini, J. E., Suh, N. P., Waldman, F. A.*
2 *Kumar, V., Suh, N. P.:* Polym. Eng. Sci. 30, p. 1323 (1990)
3 *Kumar, V.:* Ph.D. Thesis, Mechanical Engineering, Massachusetts Institute of Technology, Cambridge 1988
4 *Colton, J., Suh, N. P.:* Polym. Eng. Sci. 27, p. 493 (1987)
5 *Colton, J., Suh, N. P.:* Polym. Eng. Sci. 27, p. 485 (1987)
6 *Kweeder, J. A., Ramesh, N. S., Campbell, G. A., Rasmussen, D. H.:* SPE Tech. Papers 37, p. 1398 (1991)
7 *Ramesh, N. S., Dontula, D., Rasmussen, D., Campbell, G. A.:* SPE Tech. Papers 37, p. 11292 (1991)
8 *Kumar, V., Weller, J. E.:* SPE Tech. Papers 37, p. 1401 (1991)
9 *Kumar, V., VanderWel, M.:* SPE Tech. Papers 37, p. 1406 (1991)
10 *Kumar, V., Weller, J. E., Hoffer, H. Y.:* Symposium on Processing of Polymers and Polymeric Composites, MD-19, p. 197 (1990)
11 *Berens, A. R.:* SPE Tech. Papers 35, p. 722 (1989)
12 *Tikhomirov, B. P., Hopfenberg, H. B., Stannett, V. T., Williams, J. L.:* Makromol. Chem. 118, p. 177 (1968)
13 *Kumar, V., Weller, J. E.:* SPE Tech. Papers 38, p. 1508 (1992)
14 *Shutov, F. A.:* Integral Structural Polymer Foams. Springer, New York 1986
15 *Chow, T. S.:* Macromolecules 13, p. 362 (1980)

16 *Chiou, J. S., Barlow, J. W., Paul, D. R.:* J. Appl. Polym. Sci. 30, p. 2633 (1985)
17 *Crank, J.:* The Mathematics of Diffusion, 2nd Edition. Oxford Science Press, New York 1989

Acknowledgements

We would like to thank Paula Dunnigan of the BFGoodrich Company's Geon vinyl Division in Cleveland, Ohio, for furnishing the PVC samples used in this study. This research was supported by the National Science Foundation Grants DDM 8909104 and MSS 9114840, and a grant from the Washington Technology Centers. This support is gratefully acknowledged. Thanks also to University of Washington undergraduate students Romano Monticello, Brian Lee, Robert Lee, and Micki Nguyen for assisting in some of the experiments reported in this paper.

Date received: February 10, 1992
Date accepted: June 19, 1992